A. Narula, J.D. Biggs
Fault-Tolerant Station-Keeping on Libration Point Orbits
Journal of Guidance Control and Dynamics, Vol. 41, N. 4, 2018, p. 879-887
doi:10.2514/1.G003115

Fault-tolerant Station-keeping on Libration Point Orbits

Narula A. [1] and Biggs J.D.[2]
Politecnico di Milano, Via La Masa 34 - 20156 Milano, Italy

This paper extends a Linear Quadratic Regulator (LQR) based control scheme for station-keeping on Libration Point Orbits to enable continued tracking in the event of thruster failure. In the first instance it is shown that by using an extended state observer the fault (and disturbances) can be measured and compensated for at each sampling period using continuous thrust. It is proved that this control yields asymptotic tracking to a small bounded region around the desired reference orbit in the presence of these uncertainties. In addition, it is demonstrated that by combining this method with a sliding mode or an adaptive control, asymptotic tracking can be achieved. An advantage of this method is that the required gain for asymptotic tracking of the sliding mode component is much smaller than traditional methods; the gain magnitude is required to be larger that the magnitude of the disturbance estimation error rather than the magnitude of the disturbance. A comparison of the controllers performance against an LQR control scheme is undertaken in an application to low-thrust station-keeping on a halo orbit in the Earth-Moon-Spacecraft system in the presence of disturbances and various thruster faults.

---

[1] MSc, Department of Aerospace Science & Technology, Politecnico di Milano, Milano
[2] Associate Professor, Department of Aerospace Science & Technology, Politecnico di Milano, Milano.

Nomenclature and Symbols

$AAUMC$ = Adaptive active uncertainty measurement control

$AUMC$ = Active uncertainty measurement control

$AUSMC$ = Active uncertainty sliding mode control

$CR3BP$ = Circular restricted three body problem

$E\text{-}M$ = Earth Moon system

$ER3BP$ = Elliptical restricted three body problem

L_2 = Lagrangian Point L2

LOE = Loss of effectiveness

STM = State transition matrix

OBC = On-board computer

EPS = Electric power sub-system

β = Gain of ESO

$A(t)$ = State transition matrix

ϵ = Error in error state

η = Parameter of Sliding mode control

$\boldsymbol{f}$ = Disturbance vector (m/s^2)

$\boldsymbol{U}$ = control input (m/s^2)

$\boldsymbol{u_c}$ = commanded control vector (m/s^2)

$\boldsymbol{u}$ = linearized control input (mN)

I = Identity matrix

I. Introduction

The existing dogma of reliability driven spacecraft design can lead to inefficiencies in mass and power budgets as redundancy is built into the hardware. For example, the orbit and attitude control system would usually include back-up actuators, such as additional thrusters, in case of failure. Recently there has been an increase in interest of small spacecraft platforms such as CubeSats[1] which can accept more risk (such as by reducing the number of actuators) in order to significantly

reduce production cost. CubeSats, in particular, have seen a significant number of mission failures that have been attributed to the failure of the propulsion system. A recent study by Langer[1], described the three main subsystem failures that ultimately led to complete mission failures for CubeSats, namely, the on-board computer (OBC), the electric propulsion system (EPS) and communications. Around 19% of operational missions have resulted in failure[2] among which EPS is the most susceptible to failure with more than a 35% failure rate. The motivation of this paper is to reduce the risk of station-keeping failure due to EPS failure, not by building redundancy into the hardware but through control design.

Spacecraft station-keeping on Libration Point Orbits can be categorized into two types: (i) impulsive thrust station-keeping (usually chemical) where the controls are discontinuous and (ii) continuous, low-thrust, station-keeping (such as solar electric propulsion or solar sail spacecraft). Most of the techniques for orbit maintenance use impulsive maneuvers[3],[4],[5],[6]. For example, Xin[5] used a sub-optimal control technique (the $\theta - D$ technique) to complete the mission of multiple spacecraft formation flying in deep space about the L_2 point. Marchand and Howell[6] employed feedback linearization for formation flight in the vicinity of Lagrangian points. Bai and Junkins[4] proposed a modified Chebyshev-Picard integration method for station-keeping of L_2 Halo orbits in the Earth-Moon system. Karimi[7] solved the problem of Halo orbit control using optimal control theory and the extension of the active disturbance rejection technique to counter the external disturbances in the unstable orbit near the co-linear points.

In this paper, the focus is placed on the use of continuous thrust technologies such as electric or solar based propulsion. The computation of fuel efficient thrust for station-keeping on Halo orbits is demonstrated in [8] using classical LQR where the controls are assumed to act continuously. In addition LQR has been used for continuous thrust station-keeping using solar sails where the control inputs are nonlinear functions of the sail angles, for example, in Biggs and McInnes[9],[10]. Field-emission electric propulsion was used for station-keeping by Giorgio[11] for a preliminary study of early warning missions. However, none of these controls have considered the possibility of stabilizing the orbits in the presence of partial thruster failure. To this end an extension of LQR is developed by using an extended state observer to estimate and compensate the disturbances and

the presence of any fault in the control design at each sampling period. The control is also combined with a sliding mode and an adaptive control to guarantee asymptotic tracking in the presence of partial faults. Extended State Observers (ESO) have been used in the past to estimate disturbances and compensate for these disturbances in the control to improve the tracking error. This has been demonstrated in an application to attitude tracking in the presence of disturbances and uncertainties in the principal moments of inertia and reaction wheel friction[12, 13]. A sliding mode controller was also designed by Goddard[14] for external disturbances and fault-tolerant compensation. Recently, adaptive control has also been used for compensating disturbances for coordination and control of a formation of spacecrafts. Wang[15] designed two robust adaptive control schemes for formation keeping of a pair of satellites for which the disturbance was assumed bounded by a known nonlinear function scaled by an unknown constant. Lim and Bang[16] used an adaptive back-stepping control scheme to compensate for magnitude error and misalignment of the thruster for relative position tracking problem of formation flying. In this paper a simple sliding mode control and adaptive control are implemented alongside an ESO. This not only guarantees asymptotic tracking in the presence of partial faults and disturbances, but the associated gain is only required to be greater than the magnitude of the disturbance estimation error not the magnitude of the disturbance itself. This means that the sliding mode component of the control, which can lead to chattering, is less aggressive and that the magnitude of the disturbance does not need to be known apriori.

In this paper we demonstrate the use of this control in numerical simulation applied to spacecraft station-keeping of a halo orbit in the Earth-Moon-Spacecraft system in the presence of disturbances and thruster faults. The paper is presented as follows: Section II introduces different types of faults in the actuators/thrusters for modelling a real scenario of station-keeping. Furthermore, this section presents the station-keeping control algorithms and undertakes a linear stability analysis using Lyapunov functions of the error variables. Section III presents the numerical example of equations of motion and periodic reference orbits about the Earth-Moon L_2 libration point in the ER3BP. The simulation results are presented to validate the effectiveness of the new station-keeping controls for Halo orbit station-keeping against a conventional continuous linear feedback controller. Section IV concludes the paper.

II. Station-keeping Strategies with Thruster Faults

In this section we derive several station-keeping strategies for continuous control inputs in the presence of faults and external disturbances. The control strategies extend the conventional LQR approach by using an extended state observer along with either a sliding mode control or singular adaptive control to guarantee asymptotic tracking.

A. Fault-Modelling in Thrusters

This section will introduce the modelling of different types of control (thruster) faults that can be encountered in a spacecraft. These include:

1. Loss of Effectiveness (LOE) due to a decrease in the effectiveness of the thruster after a certain period of time and the input components u_i are characterized by an increase in the gain $u_i = (1 - k_i)u_{c_i}$ where u_{c_i} are the components of the commanded thrust with $0 < k_i < 1$ defining the extent of the loss.

2. Lock In Place (LIP) where all three thrusters are stuck in a particular position for a certain time period. This type of fault is characterized mathematically by, $u_i = \bar{u}_i(t_f)$ where, $\bar{u}_i$ gives the control input at any time instant t_f of failure.

3. Power Loss Fault (PLF) is a short-term, complete, failure of all thrusters but which are switched back on after a short period. This, for example, could be due to power loss during an eclipse.

From the above classification, the following general fault model is adopted:

$$\boldsymbol{u} = \boldsymbol{u_c} + E(\bar{\boldsymbol{u}} - \boldsymbol{u_c}) \tag{1}$$

where E is the failure indicator matrix for the thruster defined as, $E = \begin{bmatrix} k_1 & 0 & 0 \\ 0 & k_2 & 0 \\ 0 & 0 & k_3 \end{bmatrix}$, $\bar{\boldsymbol{u}}$ represents uncertain stuck failures for the thruster, $\boldsymbol{u_c}$ is the thruster's desired control commanded by the controller, and $\boldsymbol{u}$ is the control that is realized by the thruster.

Note that this fault model can represent outage, loss of effectiveness and stuck faults by using the parameters in Table 1.

Table 1 Parameters for thruster modelling

Fault Mode	$\bar{u}_i$	k_i
Normal	0	0
Outage	0	1
LOE	0	$0<k_i<1$
Stuck	$\bar{u}_i$	1

B. Linear Quadratic Regulator- A Conventional Approach

In order to optimize the use of propellant, an LQR control is developed considering the thruster model for the actuation of spacecraft as continuous. Typically for station-keeping problems the dynamics are highly nonlinear such as in the elliptic restricted three body problem. In some cases the control is also highly nonlinear such as in the case of a solar sail [9], [10] and a traditional approach is to first linearize the nonlinear system of the form:

$$\ddot{\boldsymbol{X}}_1 = g(\dot{\boldsymbol{X}}_1, \boldsymbol{X}_1, \boldsymbol{U}) + \boldsymbol{D} \tag{2}$$

where $\boldsymbol{X}_1, \boldsymbol{U}, \boldsymbol{D} \in \mathbb{R}^3$ where $\boldsymbol{X}_1$ is the position vector, $\boldsymbol{U}$ is a continuous control input and $\boldsymbol{D}$ are the unknown but bounded external disturbances and $g(\dot{\boldsymbol{X}}_1, \boldsymbol{X}_1, \boldsymbol{U})$ is a known nonlinear function. Expanding the phase space, Eq. 2 can be written in the general form:

$$\dot{\boldsymbol{X}}(t) = f(\boldsymbol{X}, \boldsymbol{U}, \boldsymbol{D}) \tag{3}$$

where, $\boldsymbol{X} = [\boldsymbol{X_1}, \boldsymbol{X_2}]$ is the state. Linearizing the nonlinear equations by defining:

$$\boldsymbol{x} = \boldsymbol{X} - \boldsymbol{X_0} \tag{4}$$

$$\boldsymbol{u} = \boldsymbol{U} - \boldsymbol{U_0} \tag{5}$$

where, $\boldsymbol{X_0}$ denotes the reference trajectory and $\boldsymbol{U_0}$ the nominal control, which yields a linear system of the form:

$$\dot{\boldsymbol{x}}(t) = A(t)\boldsymbol{x} + B\boldsymbol{u} + \boldsymbol{d} \tag{6}$$

where $\boldsymbol{x} = [\boldsymbol{x_1}, \boldsymbol{x_2}]^T$ is the error state, $\boldsymbol{x_1}$ the position error state and $\boldsymbol{x_2}$ being the velocity error state, $\boldsymbol{d} = [\mathbf{0}_{1\times 3} \quad \boldsymbol{D}]^T$ and $A(t)$ is of the form:

$$A(t) = \begin{pmatrix} \mathbf{0}_{3\times 3} & I_{3\times 3} \\ C(t) & \end{pmatrix} \tag{7}$$

where $C(t)$ is a 3×6 matrix. Then including the thruster fault model Eq. 1 gives:

$$\dot{\boldsymbol{x}}(t) = A(t)\boldsymbol{x}(t) + B\boldsymbol{u_c} + \boldsymbol{f} \tag{8}$$

where, $\boldsymbol{f}$ is defined as:

$$\boldsymbol{f} = [\mathbf{0}_{1\times 3} \quad \boldsymbol{D} + BE(\bar{\boldsymbol{u}} - \boldsymbol{u_c})]^T \tag{9}$$

In the case $\boldsymbol{f} = [\mathbf{0}_{1\times 6}]^T$ the control

$$\boldsymbol{u}(t) = -R^{-1}B^T S(t)\boldsymbol{x} \tag{10}$$

where $S(t)$ is obtained by solving the following Ricatti equation,

$$\dot{S} + SA + A^T S - SBR^{-1}B^T S + Q = 0 \tag{11}$$

is known to minimize the cost function:

$$J = \int_{t_0}^{t_f} [\boldsymbol{x}(t)^T Q \boldsymbol{x}(t) + \boldsymbol{u}(t)^T R \boldsymbol{u}(t)]dt. \tag{12}$$

However, in general $\boldsymbol{f} \neq [\mathbf{0}_{1\times 6}]$, thus an LQR control of the form Eq. 10 is not optimal in the presence of faults or disturbances.

C. Active Uncertainty Measurement Control

In this section an ESO is fused with an LQR controller to improve the tracking error when there are thruster faults or uncertain disturbances. Defining the estimator state as, $\hat{\boldsymbol{x}} = [\hat{\boldsymbol{x}}_{\boldsymbol{1}}, \hat{\boldsymbol{x}}_{\boldsymbol{2}}]^T$ and assuming that the trajectory does not deviate far from the reference trajectory, it is possible to use the linear dynamics to estimate the unknown $\boldsymbol{f}$ using the following extended state observer[17]:

$$\begin{aligned} \dot{\hat{\boldsymbol{x}}}_1 &= \hat{\boldsymbol{x}}_2 + \beta_1(\boldsymbol{x_1} - \hat{\boldsymbol{x}}_1) \\ \dot{\hat{\boldsymbol{x}}}_2 &= \hat{\boldsymbol{x}}_3 + \beta_2(\boldsymbol{x_1} - \hat{\boldsymbol{x}}_1) + C(t)\boldsymbol{x} + B\boldsymbol{u_c} \\ \dot{\hat{\boldsymbol{x}}}_3 &= \beta_3(\boldsymbol{x_1} - \hat{\boldsymbol{x}}_1) \end{aligned} \tag{13}$$

where $C(t)$ is the known 3×6 matrix in Eq. 7, β_i are the gains of the observer and $\hat{\boldsymbol{x}}_3 = \hat{\boldsymbol{f}}$ is the estimation of the unknown part of the Eq. 8. A parameterization based tuning method was employed [18] which makes the controller parameters a function of a single variable, the loop-gain bandwidth, which greatly simplifies the tuning process. Moreover, the gains are defined in terms of the controller bandwidth, ω_c, and observer bandwidth, ω_o and then ω_c set to a multiple of ω_o which in this paper is set to $\omega_o = 4\omega_c$ and therefore

$$\beta_1 = 3\omega_o, \beta_2 = 3{\omega_o}^2, \beta_3 = {\omega_o}^3. \tag{14}$$

Then by combining the linearized equations of motion in Eq. 6 with an additional variable $\boldsymbol{\zeta}$ defined by:

$$\dot{\boldsymbol{f}} = \boldsymbol{\zeta} \tag{15}$$

and defining the error in estimation as $\boldsymbol{E} = \boldsymbol{x} - \widehat{\boldsymbol{x}}$ and using Eq. 8, 13 and 15, the following closed-loop estimation error dynamics are obtained:

$$\begin{aligned} \dot{\boldsymbol{E}}_1 &= \boldsymbol{E}_2 - 3\omega_0 \boldsymbol{E}_1 \\ \dot{\boldsymbol{E}}_2 &= \boldsymbol{E}_3 - 3\omega_0^2 \boldsymbol{E}_1 \\ \dot{\boldsymbol{E}}_3 &= -3\omega_0 \boldsymbol{E}_1 + \boldsymbol{\zeta} \end{aligned} \tag{16}$$

Lemma II.1. *If $\boldsymbol{\zeta}$ is assumed to bounded as $|\boldsymbol{\zeta}| \leq \Delta$, then a scalar δ_i exist such that as the time $t \to \infty$, the estimation error converges to a bound $\| \boldsymbol{E}_i \| \leq \delta_i$, $i = 1, 2, 3$ where $\delta_i = \circ(\frac{1}{{\omega_o}^n})$ with $\circ(*)$ representing the order of the function.*

Proof. See [12, 13] for the proof. □

From this Lemma it is possible to state the following control law.

Lemma II.2. *The control $\boldsymbol{u} = \boldsymbol{u}_c - B^* \hat{\boldsymbol{x}}_3$ where $\boldsymbol{u}_c = -K\boldsymbol{x}$ then $\boldsymbol{x} = 0$ is asymptotically stable in Eq. 6 as $\omega_c \to \infty$, with B^* being the pseudo-inverse of B.*

Proof. Defining the Lyapunov function:

$$V = \frac{1}{2} \boldsymbol{x}^T \boldsymbol{x} \tag{17}$$

$$\dot{V} = \boldsymbol{x}^T \dot{\boldsymbol{x}}$$

$$= \boldsymbol{x}^T (A\boldsymbol{x} + B\boldsymbol{u_c} + \boldsymbol{f})$$

$$= \boldsymbol{x}^T (A - BK)\boldsymbol{x} - \boldsymbol{x}^T \widehat{\boldsymbol{f}} + \boldsymbol{x}^T \boldsymbol{f})$$

Defining the error in estimation as $\boldsymbol{e} = \boldsymbol{f} - \hat{\boldsymbol{f}}$ results in the following Lyapunov derivative,

$$\dot{V} = \boldsymbol{x}^T (A - BK)\boldsymbol{x} + \boldsymbol{x}^T (-\widehat{\boldsymbol{f}} + \boldsymbol{f})$$

$$\leq \boldsymbol{x}^T (A - BK)\boldsymbol{x} + |\boldsymbol{x}|\,|\boldsymbol{e}|$$

where $|\boldsymbol{x}| = \boldsymbol{x}^T \text{sign}(\boldsymbol{x})$. Now, if the controller poles tend to ∞ with $t \to \infty$, i.e. $\omega_c \to \infty$, the error in the state estimation tends to 0, i.e. $|\boldsymbol{e}| \to 0$, then, $\dot{V} < 0$, except at the desired zero state. □

Note that in practise ω_c will be constrained, so that asymptotic stability cannot be achieved in practise. The best one could expect is that the trajectory converges to a small bounded region of the reference trajectory. However, by combining ESO with a sliding mode or singular adaptive control it is possible to achieve asymptotic tracking in the presence of disturbances and faults.

D. Active Uncertainty Sliding Mode Control

The controller derived in this section is an extension to the AUMC control, with the addition of a sliding mode component. The sliding surface is defined as a function of the error in the system's state. It can be directly related to either just the position error state or both position and velocity error state. Moreover, the function $\boldsymbol{\sigma}$ is selected in such a way that it is vanishing as time $t \to \infty$. This will give rise to a stable differential equation and thus the error will also tend to 0. The following model for sliding surface is adopted:

$$\boldsymbol{\sigma} = (\frac{d}{dt} + a)^k \boldsymbol{x} \tag{18}$$

with a defines the unique pole of reduced dynamics of the system when it is in sliding mode. For this case, $k = 0$, thus making it dependent only on the position state.

A control action is defined such that it steers the system into the sliding surface manifolds such that $|\boldsymbol{\sigma}| \to 0$. The control law for AUSMC is thus developed as,

$$\boldsymbol{u}_{AUSMC} = -K\boldsymbol{x} - B^* \hat{\boldsymbol{f}} - \eta \text{sign}(\boldsymbol{\sigma}) \tag{19}$$

η is chosen as the upper bound of the disturbance to account for the problem of exceeding the limited disturbance.

In this section, a stability proof is developed to show that the AUSMC control law given by Equation 19 guarantees asymptotic stabilization of the reference trajectory.

Theorem II.3. *For the Eq. 6 with the control laws in Eq. 19, then the error state,* $|\boldsymbol{x}| \to 0$ *as* $t \to \infty$ *with the assumption that* $\eta > |\boldsymbol{e}|$.

Proof. Consider the following Lyapunov function for the above defined problem,

$$V = \frac{1}{2}\boldsymbol{x}^T\boldsymbol{x} = \boldsymbol{x}^T\dot{\boldsymbol{x}}$$

$$= \boldsymbol{x}^T(A\boldsymbol{x} + \boldsymbol{x}^T B\boldsymbol{u_c} + \boldsymbol{f})$$

$$= \boldsymbol{x}^T(A - BK)\boldsymbol{x} - \boldsymbol{x}^T\widehat{\boldsymbol{f}} - \boldsymbol{x}^T\eta\text{sign}(\boldsymbol{\sigma}) + \boldsymbol{x}^T\boldsymbol{f}$$

now if $k = 0$, $\boldsymbol{\sigma} = \boldsymbol{x}$, hence, the Lyapunov function becomes:

$$\dot{V} = \boldsymbol{x}^T(A - BK)\boldsymbol{x} + \boldsymbol{x}^T(-\widehat{\boldsymbol{f}} + \boldsymbol{f}) - \eta\boldsymbol{x}^T\text{sign}(\boldsymbol{x}) \tag{20}$$

and with $\boldsymbol{e} = \boldsymbol{f} - \hat{\boldsymbol{f}}$ gives

$$\dot{V} \leq \boldsymbol{x}^T(A - BK)\boldsymbol{x} + |\boldsymbol{x}|\,|\boldsymbol{e}| - \eta\,|\boldsymbol{x}| \tag{21}$$

As the estimation error is upper bounded then η can be chosen to be greater than this bound and it follows from the Barbalat's lemma, the system is asymptotically stable. As K is chosen such that $A - BK$ is negative definite. Then, the choice of η is such that $\eta > |\boldsymbol{e}|$, it will result a negative value of derivative of Lyapunov function, i.e. $\dot{V} < 0$ □

The sliding mode control formulation derived in this problem has a discontinuous control component which may result in high frequency switching (known as chattering) when the system is operating in a region very close to the sliding mode.

There have been many methods adopted to avoid chattering in sliding mode control, but Bharat[19] developed a simpler saturation function for the station-keeping problem. It can be used in place of sign function, to avoid excessive station-keeping cost. Defining the saturation function as:

$$sat\left(\frac{\sigma_i}{\epsilon}\right) = \left\{ \begin{array}{c} \left(\frac{\sigma_i}{\epsilon}\right), \left|\frac{\sigma_i}{\epsilon}\right| \leq 1 \\ sign\left(\frac{\sigma_i}{\epsilon}\right), \left|\frac{\sigma_i}{\epsilon}\right| > 1 \end{array} \right\} \tag{22}$$

where, σ_i is again a sliding surface as defined in Eq. 18 and ϵ is the boundary layer below which the saturation function varies continuously as per the above definition. The large value of the bound ϵ decreases the station-keeping costs but increases the station-keeping error. Therefore, a trade-off is made while choosing the value of ϵ. The values for these bounds should be chosen to keep the station-keeping costs low without sacrificing position accuracy despite the presence of significant uncertainties.

E. Adaptive Active Uncertainty Measurement Control

Another modified control strategy is proposed that can provide asymptotic tracking of a reference orbit in the presence of faults(disturbances). The principle behind this controller is to add an adaptive parameter for the control to provide tracking for the uncertain disturbances and faults. However, this adaptive parameter is unbounded and possess a singularity as $t \to \infty$. This causes problems when tracking over large time periods as the gain and corresponding required control input become too large. It can be managed by implementing a saturation block similarly to the one in AUSMC.

The adaptive control law is defined as:

$$\boldsymbol{u}_{AAUMC} = \frac{-K\boldsymbol{x}}{\sigma} - B^*\hat{\boldsymbol{f}} \tag{23}$$

with the scalar σ defined by

$$\dot{\sigma} = \frac{d\sigma}{dt} = \left\{ \begin{array}{ll} \frac{-k\sigma \boldsymbol{x}^T sign(\boldsymbol{x})}{\|\boldsymbol{x}\|^2}, & \boldsymbol{x} \neq 0 \\ 0, & \boldsymbol{x} = 0 \end{array} \right. \tag{24}$$

where $\sigma(0) > 0$ and $\dot{\sigma}(0) < 0$. Here, the adaptive feedback controller with ESO can compensate for the estimation error rather than the entire disturbance and can track a prescribed reference trajectory such that the closed-loop system is stable. A stability proof shows that the AAUMC control law given in Eq. 23 guarantees asymptotic stabilization of the system.

Theorem II.4. *For the system given in Eq. 6 with the adaptive control law in Eq. 23 with* $0 < \sigma \leq 1$ *defined in Eq. 24 yields* $|\boldsymbol{x}| \to 0$ *as* $t \to \infty$.

Proof. Consider the following Lyapunov function for the above defined problem,

$$V = \frac{\sigma^2}{2}\boldsymbol{x}^T\boldsymbol{x} \tag{25}$$

Taking the derivative of the Lyapunov function:

$$\dot{V} = \sigma^2\boldsymbol{x}^T\dot{\boldsymbol{x}} + \sigma\dot{\sigma}\boldsymbol{x}^T\boldsymbol{x}$$

$$= \sigma^2\boldsymbol{x}^T(A\boldsymbol{x} + B\boldsymbol{u_c} + \boldsymbol{f}) + \sigma\dot{\sigma}\boldsymbol{x}^T\boldsymbol{x}$$

Here, $\boldsymbol{u_c}$ is replaced by $\boldsymbol{u}_{AAUMC}$ as defined in Eq. 23.

$$\dot{V} = \sigma^2\boldsymbol{x}^T(A - B\frac{K}{\sigma})\boldsymbol{x} - \sigma^2\boldsymbol{x}^T\widehat{\boldsymbol{f}} + \sigma^2\boldsymbol{x}^T\boldsymbol{f} + \sigma\dot{\sigma}\boldsymbol{x}^T\boldsymbol{x}$$

$$= \sigma\boldsymbol{x}^T(A\sigma - BK)\boldsymbol{x} - \sigma^2\boldsymbol{x}^T\widehat{\boldsymbol{f}} + \sigma^2\boldsymbol{x}^T\boldsymbol{f} + \sigma\dot{\sigma}\boldsymbol{x}^T\boldsymbol{x}$$

$$= \sigma\boldsymbol{x}^T(A\sigma - BK)\boldsymbol{x} + \sigma^2\boldsymbol{x}^T(-\widehat{\boldsymbol{f}} + \boldsymbol{f}) + \sigma\dot{\sigma}\boldsymbol{x}^T\boldsymbol{x}$$

where σ is defined in the Eq. 24. Also, defining the error in estimation as $\boldsymbol{e} = \boldsymbol{f} - \hat{\boldsymbol{f}}$ results in the following Lyapunov derivative,

$$\dot{V} \leq \sigma\boldsymbol{x}^T(A\sigma - BK)\boldsymbol{x} + \sigma^2|\boldsymbol{x}^T|\,|\boldsymbol{e}| + \sigma\dot{\sigma}\boldsymbol{x}^T\boldsymbol{x} \tag{26}$$

As it has been shown in Theorem II.3, that stability exist if the term $\sigma^2|\boldsymbol{x}^T|\,|\boldsymbol{e}|$ is replaced as $\sigma^2\eta\text{sign}(\boldsymbol{x})$, with $\eta > |\boldsymbol{e}|$. Therefore, in Eq. 26, the derivative of Lyapunov stability should be less that 0 with the existence of following conditions:

- $k > |\boldsymbol{e}|$
- $\dot{\sigma} = \frac{-k\sigma\boldsymbol{x}^T sign(\boldsymbol{x})}{\boldsymbol{x}\boldsymbol{x}^T}$
- Also, for $(A\sigma - BK)$ is to be negative definite, range of σ is established as $0 < \sigma \leq 1$

Thus, with these consideration stability of this controller is established, i.e. $\dot{V} < 0$ □

III. Numerical Example

In this section, the ER3BP equations are formulated to obtain periodic orbits and furthermore the simulation results of each station-keeping strategy is presented.

A. Elliptical restricted three-body problem

a. Dynamics For a ER3BP, the motion of the motion of Moon around the Earth are considered eccentric ($e = 0.0549$) rather than a circular approximation. The infinitesimal mass m_3 of spacecraft compared to the mass m_1 of the Earth and the mass m_2 of the Moon is also assumed to be negligible.

With these assumption in mind, a rotating coordinate system ($\hat{X}$,$\hat{Y}$,$\hat{Z}$) is defined with the origin set at the barycenter of the E-M system as shown in the figure 1. Non-dimensionalization is

Fig. 1 Synodic Rotating Reference Frame

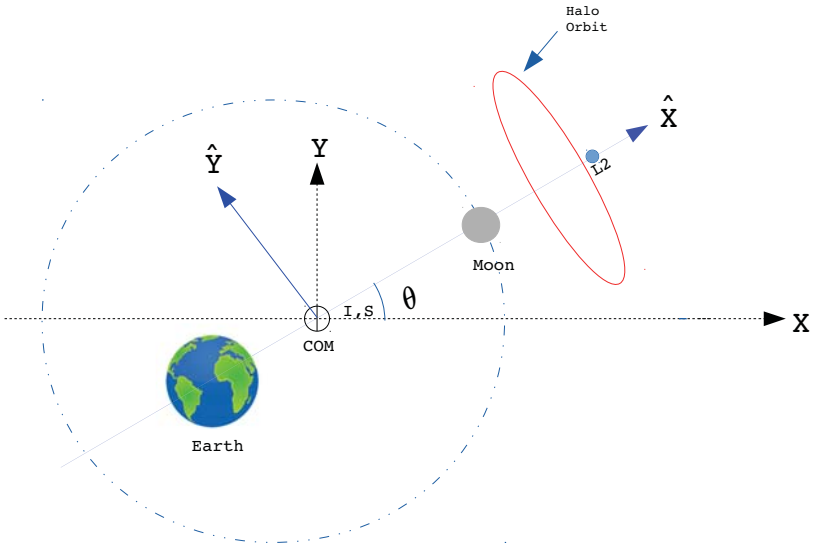

performed by defining the distance between the Earth and the Moon as the characteristics length, the time of $1/n$ as the unit of time TU, and the characteristics mass as the sum of the mass of the Earth and the Moon. Normalization is obtained by setting $\mu = \frac{m_2}{m_1+m_2}$, $m_2 = \mu$ and $m_1 = 1 - \mu$. Also, the normalized location of Earth and Moon is given as $(-\mu, 0, 0)$ and $(1-\mu, 0, 0)$ respectively. In the case of the elliptic problem, the non-dimensional angular rate and angular velocity varies

with time and is written as,

$$n = \dot{\theta} = \frac{(1 + ecos\theta)^2}{(1 - e^2)e^{\frac{3}{2}}}, \dot{n} = -2e\frac{sin\theta}{(1 - e^2)^{\frac{3}{2}}} \tag{27}$$

Then the ER3BP is described by the equation of motion:

$$\begin{aligned} \ddot{x} - 2n\dot{y} - \dot{n}y - n^2x &= -\frac{(1-\mu)(x+\mu\sigma)}{d^3} - \frac{\mu(x-(1-\mu)\sigma)}{r^3} \\ \ddot{y} + 2n\dot{x} + \dot{n}x - n^2y &= -\frac{(1-\mu)y}{d^3} - \frac{\mu y}{r^3} \\ \ddot{z} &= -\frac{(1-\mu)z}{d^3} - \frac{\mu z}{r^3} \end{aligned} \tag{28}$$

where,

$$\begin{aligned} \boldsymbol{d} &= (x + \mu\sigma)\hat{X} + y\hat{Y} + z\hat{Z}, \\ \boldsymbol{r} &= (x - (1 + \mu)\sigma)\hat{X} + y\hat{Y} + z\hat{Z}, \\ \sigma &= \frac{1 - e^2}{1 + ecos\theta} \end{aligned} \tag{29}$$

b. Periodic Orbits Among all the equilibrium points in the Earth-Moon system, L_2 lagrangian point is taken into consideration to achieve best visibility and communication with the Earth and the Moon. These periodic solutions are initially presented by Richardson [20] and have been widely quoted and used.

The choice of orbit was motivated with the coverage of south pole by various L_2 orbits. Orbit with following initial condition is used for this problem as it can provide around 90% coverage in most location of interest on the moon.

$$\begin{bmatrix} x_0 \\ y_0 \\ z_0 \\ \dot{x}_o \\ \dot{y}_0 \\ \dot{z}_0 \end{bmatrix} = \begin{bmatrix} 1.13424283994529 \\ 0 \\ 0.187435048916681 \\ 0 \\ -0.223784191244108 \\ 0 \end{bmatrix} \tag{30}$$

Table 2 Simulation Parameters

Parameters	Values
Injection Errors	δX=100 Km, δV=1 m/s
LQR Gains	Q = diag(1,1,1,100,100,100), R = diag(0.04,0.04,0.04)
AUMC Observer Gains	β_1=30, β_2=300, β_3=1000
AUSMC Parameters	a=2.599e-05, ϵ=1e-3, η=diag(0.01,0.01,0.01)
AAUMC Parameters	k=0.01

B. Simulation Results

Min Zhu[21] in his work on active disturbance rejection control identified the following important parameters to study the performance of station-keeping strategies implemented on the satellite. The velocity increments ΔV (in unit of $m/s/T$) , and the mean absolute value of the position errors e_x, e_y & e_y are defined as followed:

$$\begin{aligned} \Delta V_i &= \frac{1}{T}\int_0^T |u_i|\, dt \\ \Delta V &= \sqrt{\Delta V_x^2 + \Delta V_y^2 + \Delta V_z^2} \\ e_i &= |\Delta i|_{mean} \\ \Delta e &= \sqrt{e_x^2 + e_y^2 + e_z^2} \end{aligned} \tag{31}$$

with $i = x, y, z$

Another parameter that could be effective in defining the performance of control is the convergence time. It is defined as the time taken by position or velocity error to converge to a certain value from the time they occur.

Since, CubeSat will have a ride-share mission to moon aboard another spacecraft, there is a possibility to experience high injection errors. For simulation purposes, initial conditions are perturbed from the nominal values that are used in the reference orbit. For the simulation purpose, values in table 2 of each of the parameters are used in dimensionless coordinates.

1. Station-keeping with injection and tracking errors

Figure 2 highlights the results of halo orbits control force encountered due to the presence of injection error of 100 Km for the AUMC, AUSMC and AAUMC control with respect to the LQR control. It can be seen from the table 3 that AUMC has a negligible decrease in position errors but it is faster in convergence as compared to LQR.

Table 3 Performance parameters for Controls with Injection Errors

Control Strategy	ΔV (m/s/T)	Δe (km)	Convergence time(days)
LQR	5.8432	30.86	27.117
AUMC	5.8238	29.55	17.027
AUSMC	5.7001	26.24	9.365
AAUMC	5.9316	22.46	13.207

It takes around 17.027 days as compared to 27.117 days for LQR which is about of 37.2% decrease in convergence time while the error is just decreased by 4.2%. In case of AUSMC and AAUMC position error is reduced by 14.9% and 27.2%, while there is above 50% which is high improvement in convergence time as compared to LQR. It can be seen that ΔV is almost same throughout all the three strategy with very little variation in it.

2. Station-keeping with thrusters fault

There are three fault scenarios simulated as discussed in the section II A such as faults due to power outage, thruster stuck and loss of effectiveness.

a. Thruster outage: The following values in table 4 were chosen for the parameters $\bar{\boldsymbol{u}}$ and E to simulate this fault. Figure 3 underlines the effects for each of station-keeping strategy for required control thrust with respect to LQR. As expected AUSMC has the lowest convergence time of 12.14 as compared to LQR of 20 days staying in almost the same range of ΔV for both. But, a position error improvement of 9.93%, 16.4% and 13.3% is seen in AUMC, AUSMC and AAUMC with respect to LQR. Table 5 can be referred for the effect of position error and time of convergence for the fault.

Fig. 2 Thrust comparison with injection errors

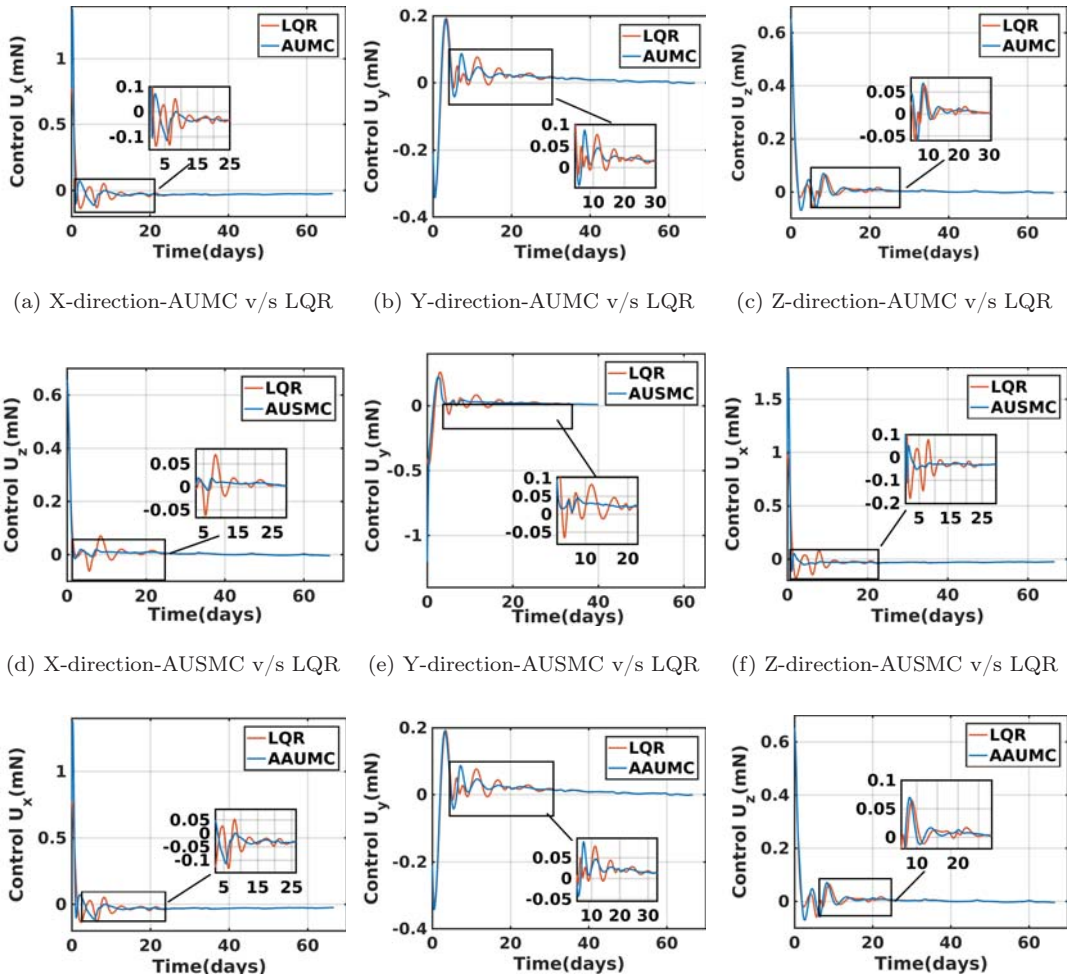

(a) X-direction-AUMC v/s LQR (b) Y-direction-AUMC v/s LQR (c) Z-direction-AUMC v/s LQR

(d) X-direction-AUSMC v/s LQR (e) Y-direction-AUSMC v/s LQR (f) Z-direction-AUSMC v/s LQR

(g) X-direction-AAUMC v/s LQR (h) Y-direction-AAUMC v/s LQR (i) Z-direction-AAUMC v/s LQR

Table 4 Thruster Outage Parameters

Parameter	**Value**
$\bar{u}$	0
E	diag(1,1,1)
Out time	4.32 days

b. Thruster Stuck: In order to simulate this scenario, it is assumed that the thrust is stuck at 60% capacity of its maximum capability for the duration of around 5 days due to lack of required power. This time duration is considered as 5 days keeping maximum eclipse time that the spacecraft will encounter in this orbit. The effects can be seen in table 6.

Table 5 Thruster Outage Fault of including Injection errors and Thruster Outage faults

Control Strategy	ΔV (m/s/T)	Δe (km)	Fault Convergence time(days)
LQR	15.447	59.032	>20
AUMC	15.427	53.360	19.41
AUSMC	14.859	47.516	12.14
AAUMC	14.24	52.201	18.01

Table 6 Thruster stuck fault including Injection errors and Thruster stuck faults

Control Strategy	ΔV (m/s/T)	Δe (km)	Fault Convergence time(days)
LQR	7.846	43.18	8.91
AUMC	7.992	40.66	8.596
AUSMC	7.759	37.787	7.666
AAUMC	8.013	32.86	8.469

c. Loss of Effectiveness: The values in table 5 were chosen for the parameters $\bar{u}$ and e to simulate this fault.

Table 7 Thruster LOE Parameters

Parameter	**Value**
$\bar{\boldsymbol{u}}$	0
E	diag(0.4,0.3,0.6)
Out time	4 days

This is the important result that shows prominent effect of the controller developed by addition of sliding surface to an observer. The main effect can be seen in case of AUSMC, the error remains much bounded to almost ignore the convergence of this control and thus reducing the requirement of extra control efforts. Table 8 shows the effect for this case. As always the ΔV are in the same order for all four cases but slight improvement is seen for the position errors. It can be seen that

Fig. 3 Thrust comparison with injection errors and outage faults

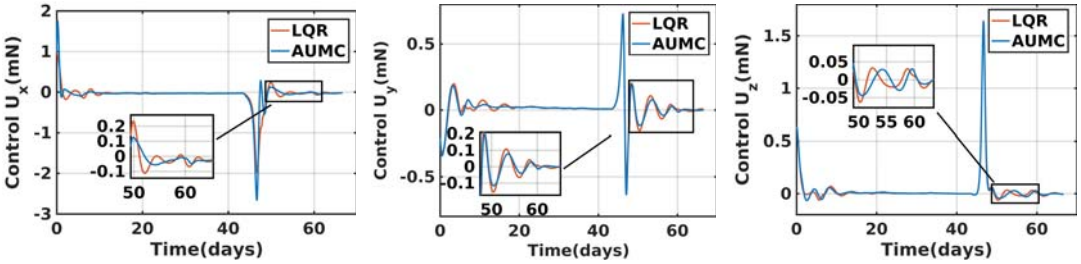

(a) X-direction-AUMC v/s LQR (b) Y-direction-AUMC v/s LQR (c) Z-direction-AUMC v/s LQR

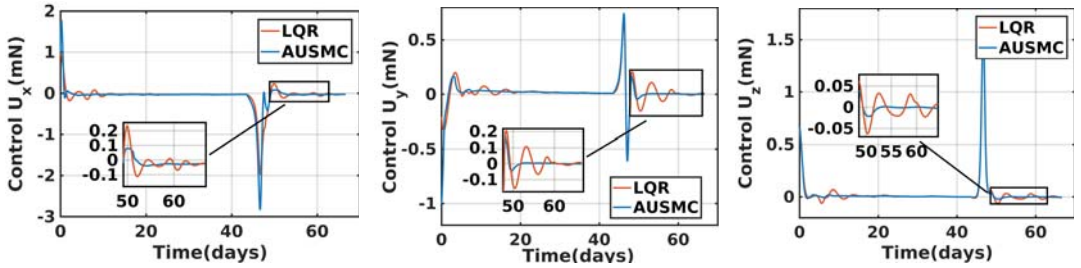

(d) X-direction-AUSMC v/s LQR (e) Y-direction-AUSMC v/s LQR (f) Z-direction-AUSMC v/s LQR

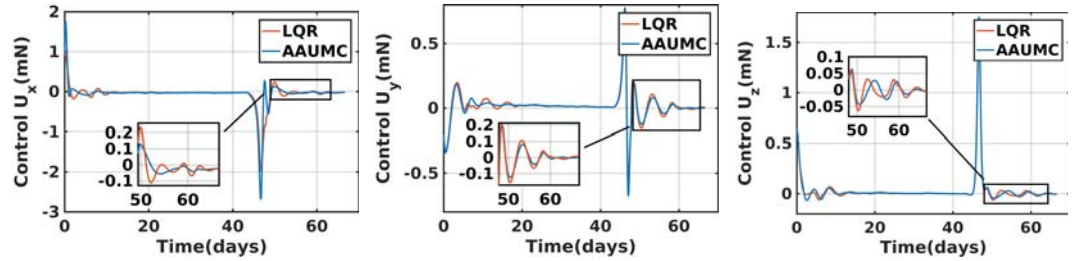

(g) X-direction-AAUMC v/s LQR (h) Y-direction-AAUMC v/s LQR (i) Z-direction-AAUMC v/s LQR

there is just a 12% decrease in fault convergence time for AUSMC as compared to LQR.

Table 8 Thruster LOE fault including Injection errors and thruster LOE faults

Control Strategy	ΔV (m/s/T)	Δe (km)	Fault Convergence time(days)
LQR	7.621	33.92	6.14
AUMC	7.440	32.76	5.81
AUSMC	7.396	30.83	1.15
AAUMC	7.652	31.78	5.45

The simulation results show that it is feasible for a 6U CubeSat with, for example, a field

emission electric propulsion system to stabilize its motion on a halo orbit in the Earth-Moon-Spacecraft system even with the presence of certain faults, typical environmental disturbances and injection errors.

IV. Conclusion

Linear Quadratic Regulator (LQR) based controllers have been proposed for fuel-efficient station-keeping missions about Libration point orbits. These controls are simple to implement and optimal provided the spacecraft does not drift too far from the reference orbit. In this paper LQR is extended to include a simple linear extended state observer that is shown to improve the station-keeping tracking performance in the presence of disturbances and thruster faults. For example, with orbital injection errors of 100 km in position and 1 m/s in velocity the extended control stabilizes the satellite's orbit in approximately 17 days whereas using LQR alone takes approximately 27 days for convergence.

Despite the improvement in the simulation example, the mathematical proof of asymptotic stability could only be demonstrated under the assumption of perfect estimation of the faults and disturbances. It was then demonstrated that by coupling this control with a sliding mode component or a singular adaptive gain that asymptotic tracking can be achieved in the presence of faults and disturbances. Moreover, the control coupled with the sliding mode component, called the Active Uncertainty Sliding Mode Control (AUSMC), outperforms the other control algorithms in terms of convergence time with faults and disturbances. For instance, with a power outage for 4 days, the AUSMC control scheme takes approximately 12 days to stabilize the satellite's orbit as compared to approximately 20 days in the case of an LQR control.

The simulation results also show that it is feasible for a 6U CubeSat with continuous low-thrust electric propulsion (with a maximum thrust of approximately 2.5 mN) to undertake station-keeping on Libration point orbits in the presence of partial or complete short-term faults and disturbances.

V. Appendix

Figure 4 and 5 represent the results of station-keeping with thruster stuck and LOE faults.

Fig. 4 Thrust comparison with injection errors and thruster stuck faults

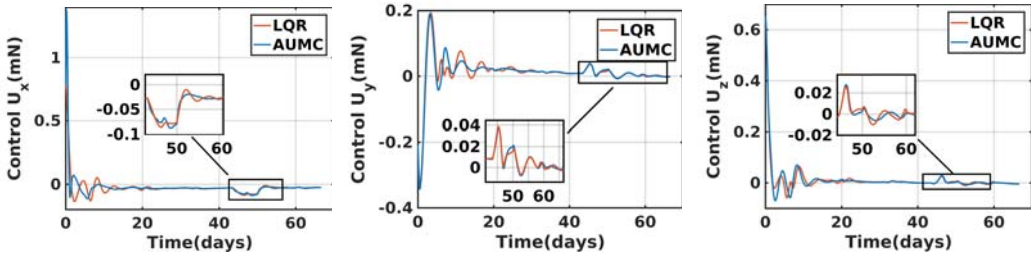

(a) X-direction-AUMC v/s LQR

(b) Y-direction-AUMC v/s LQR

(c) Z-direction-AUMC v/s LQR

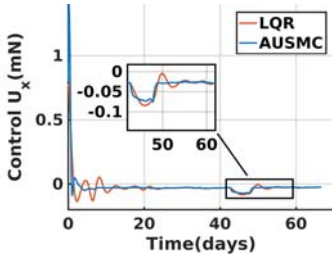

(d) X-direction-AUSMC v/s LQR

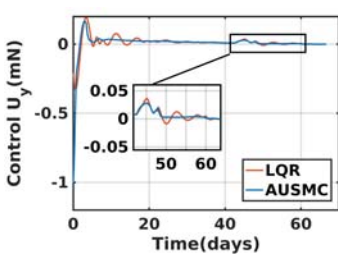

(e) Y-direction-AUSMC v/s LQR

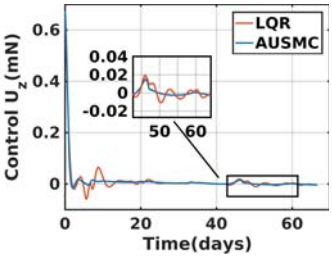

(f) Z-direction-AUSMC v/s LQR

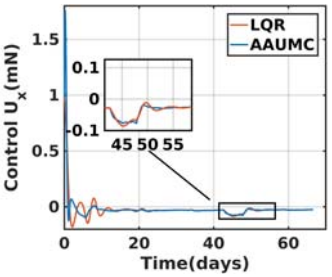

(g) X-direction-AAUMC v/s LQR

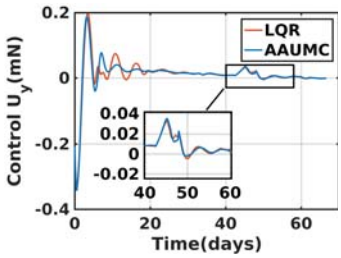

(h) Y-direction-AAUMC v/s LQR

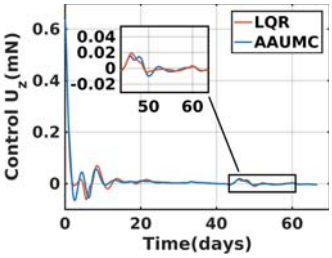

(i) Z-direction-AAUMC v/s LQR

Fig. 5 Thrust comparison with injection errors and thrusters LOE faults

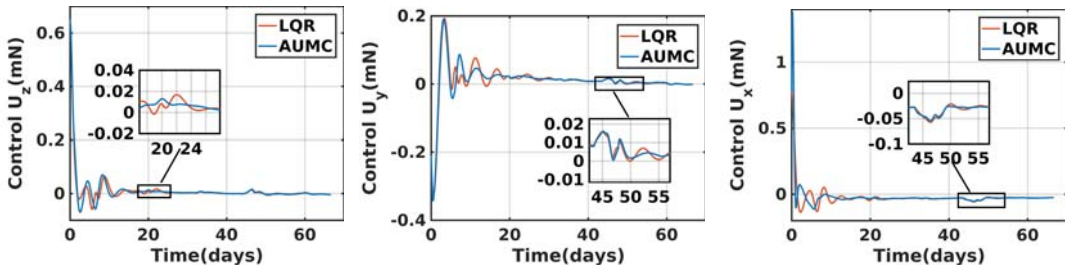

(a) X-direction-AUMC v/s LQR (b) Y-direction-AUMC v/s LQR (c) Z-direction-AUMC v/s LQR

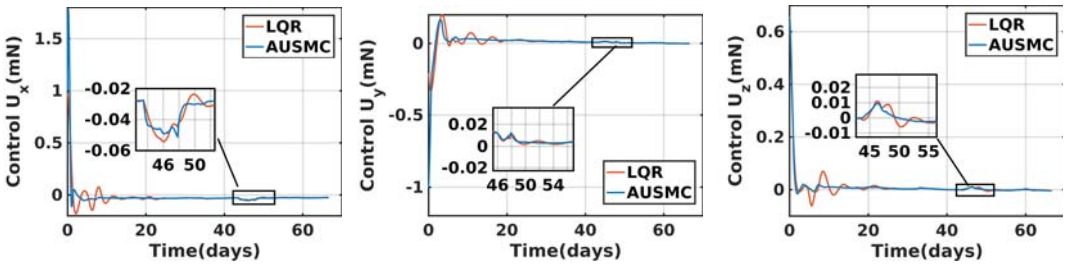

(d) X-direction-AUSMC v/s LQR (e) Y-direction-AUSMC v/s LQR (f) Z-direction–AUSMC v/s LQR

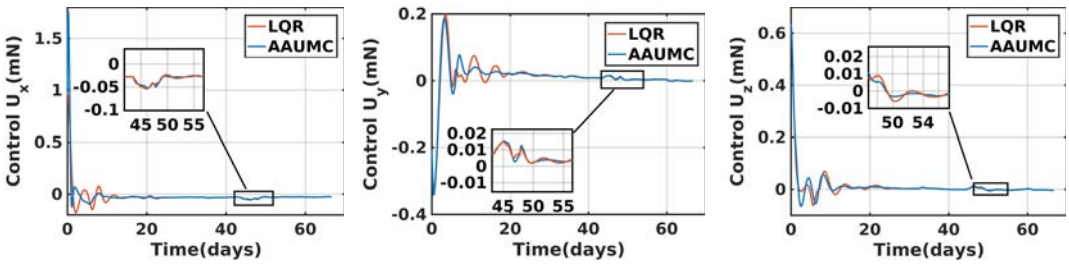

(g) X-direction-AAUMC v/s LQR (h) Y-direction-AAUMC v/s LQR (i) Z-direction-AAUMC v/s LQR

References

[1] Langer, M. and Bouwmeester, J., "Reliability of CubeSat's Statistical Data, Developers Beliefs and the Way Forward," in "30^{th} Annual AIAA Conference on Small Satellites, Technical Session X- Advanced Technologies II," , 2016.

[2] Bouwmeester, J., Langer, M., and Gill, E., "Survey on the implementation and reliability of CubeSat electrical bus interfaces," *CEAS Space Journal, Vol. 9, No. 2, pp. 163-173, 2017*, doi:10.1007/s12567-016-0138-0.

[3] Cielaszyk, D. and Wie, B., "New approach to halo orbit determination and control," *Journal of Guidance, Control, and Dynamics, Vol. 19, No. 2, pp. 266-273, 1996*, doi:http://dx.doi.org/10.2514/3.21614.

[4] Bai, X. and Junkins, J., "Modified Chebyshev-Picard Iteration Methods for Station-Keeping of Translu-

nar Halo Orbits," *Mathematical Problems in Engineering, Article ID: 926158, 18 pp., 2012*, doi:http://dx.doi.org/10.1155/2012/926158.

[5] Xin, M. and Balakrishnan, S., "A new method for sub-optimal control of a class of non-linear systems," *Optimal Control, Applications and Methods Vol. 26, Issue 2, pp. 55-83, 2005*, doi:10.1002/oca.750.

[6] Pavlak, T. and Howell, K., "Strategy for Optimal, Long-Term Libration Point Orbit Stationkeeping in the Earth-Moon System," *AAS/AIAA Astrodynamics Specialist Conference, AIAA 2012-4665, 2012*, doi:http://dx.doi.org/10.2514/6.2012-4665.

[7] Zhu, M., Karimi, H., H.Zhang, Q.Gao, and Wang, Y., "Active Disturbance Rejection Station-Keeping Control of Unstable Orbits around Collinear Libration Points," *Mathematical Problems in Engineering, Article ID: 410989, 2014*, doi:10.1155/2014/410989.

[8] Wie, B., *Space Vehicle Dynamics and Control*, AIAA Education Series, pp. 121-205, Chapter 2, 2008.

[9] Biggs, J. D. and McInnes, C. R., "Solar Sail Formation Flying for Deep-Space Remote Sensing," *Journal of Spacecraft and Rockets, Vol. 46, No. 3, pp. 670-678, 2009*, doi:http://dx.doi.org/10.2514/1.42404.

[10] Biggs, J. D., McInnes, C. R., and Waters, T., "Control of Solar Sail Periodic Orbits in the Elliptic Three-Body Problem," *Journal of Guidance, Control, and Dynamics, Vol. 32, No. 1, pp. 318-320, 2009*, doi:http://dx.doi.org/10.2514/1.38362.

[11] Giorgiani, G., "Orbital maintenance near libration points by electric propulsion: Preliminary study of Mission," in "1^{st} AIAA-Pegasus Student Conference, 2005," , 2005.

[12] Bai, Y., Biggs, J. D., Wang, X., and Cui, N., "A Singular Adaptive Attitude Control with active disturbance rejection," *European Journal of Control, 2017, pp. 50-56*, doi:https://doi.org/10.1016/j.ejcon.2017.01.002.

[13] Bai, Y., Biggs, J. D., Bernelli-Zazzera, F., and Cui, N., "Adaptive attitude tracking with active uncertainty rejection," *Journal of Guidance, Control and Dynamics, 2017, in press.*

[14] Godard, G. and Kumar, K., "Fault Tolerant Reconfigurable Satellite Formations Using Adaptive Variable Structure Techniques," *Journal of Guidance, Control, and Dynamics, Vol. 33, No. 3 (2010), pp. 969-984, 2010*, doi:http://dx.doi.org/10.2514/1.38580.

[15] Wang, Z., Khorrami, F., and Grossman, W., "Robust Adaptive Control of Formation keeping for a Pair

of Satellites," *Proceedings of the American Control Conference, Vol. 2, IEEE Publ., Piscataway, NJ, pp. 834-838, 2000*,
doi:10.1109/ACC.2000.876616.

[16] Lim, H. and Bang, H., "Adaptive Control for Satellite Formation Flying Under Thrust Misalignment," *Acta Astronautica, Vol. 65, No. 1-2,pp. 112-122, 2009*,
doi:https://doi.org/10.1016/j.actaastro.2009.01.022.

[17] Chen, X., Li, D., Gao, Z., and Wang, C., "Tuning method for second-order active disturbance rejection control," *Proceedings of the* 30^{th} *Chinese Control Conference, pp. 6322-6327, 2013.*

[18] Gao, Z., "Scaling and Parametrization Based Controller Tuning," *Proceedings of the American Control Conference, Vol. 6, pp. 4989-4996, 2003*,
doi:10.1109/ACC.2003.1242516.

[19] Mahajan, B., "Libration point orbits near small bodies in the elliptic restricted three-body problem," *Master Thesis, 2013.*